2012 IEEE/RSJ International Conference on
Intelligent Robots and Systems
October 7-12, 2012. Vilamoura, Algarve, Portugal

A Nonlinear Path Following Controller for an Underactuated Unmanned Surface Vessel

John M. Daly, Michael J. Tribou, and Steven L. Waslander

Abstract— **This work presents a novel path following controller for underactuated unmanned surface vessels (USVs) that is both provably stable and intuitive to tune. The approach consists of a navigation component that computes a desired heading angle to ensure the USV will arrive at the path, and a nonlinear controller to guarantee exponential tracking of surge velocity and heading. Additionally, ultimate boundedness of the unactuated sway velocity is proven. Simulation results are presented to show numerically that the controller works as expected in the ideal case. Outdoor experimental results are presented, using a GPS and compass as sensors, showing the practical feasibility of the approach in the presence of sensor noise, disturbances, and unmodeled dynamics.**

Index Terms— **Mobile robotics, path following control, surface vessel, navigation.**

I. Introduction

Unmanned surface vessels (USVs) are finding use in a variety of applications, including environmental monitoring and surveillance. Many of the mechanical designs are such that these systems are underactuated, often having only two control inputs for three or more degrees of freedom (DOF), which presents an additional challenge in control over a fully-actuated plant. When attempting control of such plants, a variety of objectives such as trajectory tracking, dynamic positioning, and path following may be considered. This work examines the path following problem for underactuated USVs and presents a novel approach that is both provably stable and straightforward for the practitioner to tune. By designing a control law that contains terms to cancel out the nonlinearities in the USV dynamics along with a set of stabilizing control terms in the form of a PID controller for the heading angle and a PI controller for the surge speed, a stabilizing and intuitive control law is obtained.

A number of researchers have examined the modeling and control problems for USVs, e.g. [1], [2], [3]. The specific problem of path following with underactuated USVs has also received significant attention in the literature. In [4], Fossen *et al.* present a controller to accomplish the path following task. The controller is derived using a Lyapunov analysis, and contains nonlinear dynamic terms to stabilize the closed loop. Experimental results in a pool using an indoor positioning system are presented. While the indoor experimental results look promising, this controller is not intuitive to tune from the standpoint of a practitioner. Bibuli *et al.* [5] present a path following controller for stabilizing an underactuated USV specifically to a line path. The control law requires knowledge of the surge and sway accelerations. However, in practice they assume that the acceleration terms are a slowly varying disturbance and introduce integral action in the controller to compensate for them instead of measuring and incorporating the accelerations directly. No proof of stability is provided for the modified version of the controller implemented in practice. In [6], Bibuli *et al.* present a kinematic path following controller. Their focus is on developing a stable *kinematic* path following algorithm to generate reference surge and yaw rates to provide to a lower level controller for tracking. The dynamic controller presented in [7], consisting of gain scheduled PI controllers for surge speed and yaw rate, is used by Bibuli *et al.* to ensure tracking of the reference signals. Local stability of each controller is shown by assuming decoupling of surge and yaw and linearizing a simplified model of the dynamics about an operating point.

In this work, a control law is presented to ensure path following of continuously differentiable paths. Necessary and sufficient conditions on the choice of controller gains are given to yield exponential convergence of the yaw and the surge speed to desired values. Additionally, assuming that the first and second time derivatives of the desired yaw as well as the desired surge speed are bounded, ultimate boundedness of the unactuated sway velocity is proved. A second motivation of this work is to develop a control technique that is accessible, providing PID terms for tuning, as this is a common framework familiar to practitioners in industrial applications of USVs.

Section II presents the equations of dynamics for a USV, along with the guidance strategy and the path following controller. In Section III, a closed loop stability analysis of the proposed controller is presented. Simulation results are presented in Section IV. Outdoor experimental results are given in Section V. Conclusions are given and opportunities for future work are discussed in Section VI.

II. Path Following Controller Design

To develop a suitable provably stable nonlinear controller for the USV, it is important to begin with an accurate model of the dynamics. Krishnamurthy *et al.* [1] develop a detailed 6-DOF dynamic model for USVs operating in the sea. Particular attention is paid to disturbances such as ocean currents, waves, and wind, which are relevant effects for

John M. Daly is with Quanser Consulting Inc., 119 Spy Court, Markham, Ontario, Canada. jmdaly@gmail.com.

Michael J. Tribou is with the Department of Electrical and Computer Engineering, University of Waterloo, 200 University Avenue West, Waterloo, Ontario, Canada. mjtribou@uwaterloo.ca.

Steven L. Waslander is with the Department of Mechanical and Mechatronics Engineering, University of Waterloo. stevenw@uwaterloo.ca.

978-1-4673-1736-8/12/S31.00 ©2012 IEEE

a USV operating at sea. However, in this work, a simpler rigid body dynamic model of a USV from [8] is used. With this 3-DOF model, the first three states express the kinematic relationship between velocity in the body-fixed frame and velocity in the inertial frame. This relationship may be expressed as,

$$\dot{\eta} = R(\psi)\nu \tag{1}$$

where $\eta = [x, y, \psi]^T$ represents the position and orientation of the vehicle in the global frame and $\nu = [u, v, r]^T$ represents the x (surge) and y (sway) components of the velocity vector expressed in the body-fixed frame [8] and the angular velocity, respectively. The USV is assumed to be symmetric along the port-starboard axis, but may not be along the bow-stern axis. As a result, the parameter x_g is defined to denote the origin of the body-fixed frame from the centre of gravity along the body x axis [8]. The rotation matrix $R(\psi)$ is given as,

$$R(\psi) = \begin{bmatrix} \cos\psi & -\sin\psi & 0 \\ \sin\psi & \cos\psi & 0 \\ 0 & 0 & 1 \end{bmatrix}. \tag{2}$$

This matrix rotates vectors from the body-fixed frame into the inertial frame. The rigid body equations of motion are then given as [8],

$$M\dot{\nu} + C(\nu)\nu + D\nu = \tau \tag{3}$$

where M, $C(\nu)$, and D represent the mass, Coriolis, and damping matrices respectively. They are given as,

$$M = \begin{bmatrix} m & 0 & 0 \\ 0 & m & mx_g \\ 0 & mx_g & I_z \end{bmatrix} \tag{4}$$

$$C(\nu) = \begin{bmatrix} 0 & 0 & -m(x_g r + v) \\ 0 & 0 & mu \\ m(x_g r + v) & -mu & 0 \end{bmatrix} \tag{5}$$

$$D = \begin{bmatrix} d_{11} & 0 & 0 \\ 0 & d_{22} & 0 \\ 0 & 0 & d_{33} \end{bmatrix} \tag{6}$$

where m is the mass of the USV, I_z is the moment of inertia about the z (vertical) axis, and the diagonals of D represent damping along the surge, sway, and yaw directions respectively. In practice, the physical parameters of the dynamic model are determined by performing a system identification. The vector $\tau = [\tau_u, \tau_v, \tau_r]^T$ represents the input forces and torque. Note that since the vehicle used in this work is underactuated in the sway direction, τ_v is always zero. This complicates control design, but the next section will present a controller for the underactuated system that achieves path following and guarantees stability of the heading and velocity states.

A. Guidance

The path following problem focuses on ensuring that a vehicle will get to a path and stay on that path. Unlike trajectory tracking, there is not a requirement to have the vehicle reach certain positions at certain points in time. Instead, the goal is to traverse the path with a desired velocity. In this work, we parameterize the path of interest in x and y in the global frame with a scalar variable θ. That is, the path to follow may be expressed as $p_d(\theta) = [x_d(\theta), y_d(\theta)]^T$.

In order to accomplish path following, one must find the closest point to the USV on the path. In the case of very simple paths, one may use geometry to determine the closest point. When the path is more complicated a geometric approach may not be as straightforward. In the general case, one may formulate the problem of finding the closest point as an optimization problem and seek to find the path parameter θ that minimizes the distance of the USV to the path. Breivik and Fossen approach this problem by determining the dynamics of the path error and stabilizing this error using a Lyapunov analysis [9]. This analysis results in dynamics $\dot{\theta}(t)$ for the path parameter that may be numerically integrated online. In practice, their approach requires a high gain so that the optimal θ is reached rapidly [10]. It was determined in our work that, for the sample frequencies used in our experiments, the large gain required along with noise on the measurements lead the solution $\theta(t)$ to be numerically unstable some of the time. As a result, we propose the following general approach to find the closest point on the path to the USV. Define the position of the USV as $p(t) = [x(t), y(t)]^T$ and the distance to the path as $e(\theta) = p(t) - p_d(\theta)$. Then, define the cost function $J(\theta) = \frac{1}{2}e^T e$.

This quadratic cost function may be minimized using a gradient descent algorithm. We propose solving this gradient descent optimization at every time step. For instance, at time step t_i, one may iteratively solve for θ as,

$$\theta(k+1) = \theta(k) - \gamma \nabla J(\theta(k)) \tag{7}$$

where $\gamma > 0$ is a parameter that controls the convergence rate. It was determined experimentally that this approach yields convergence to the locally closest point on the path that is rapid enough from a computational point of view to be performed online. Additionally, it is a straightforward method that works well in the presence of measurement noise and in experiments with large sample periods.

Having determined the closest point on the path to the USV, the navigation component must then provide a desired heading for the controller to track. As with many path following problems in mobile robotics, the goal is not to point directly at the closest point on the path, but instead to point a small distance $\Delta\theta$ ahead of the closest point. This "carrot point" leads the vehicle, ensuring that it will always point further along the path, even when exactly on the path. This is a tunable parameter affecting how far ahead along the path the vehicle should point. In the future, analytic methods

for determining $\Delta\theta$ based on the desired speed and path will be investigated. The reference heading ψ_{ref} for the USV is then determined as the angle of the vector connecting the USV and the carrot point,

$$\psi_{ref} = \arctan\left(\frac{y_d(\theta+\Delta\theta) - y(t)}{x_d(\theta+\Delta\theta) - x(t)}\right). \tag{8}$$

B. Path Following Control Law

While a number of nonlinear control strategies exist for the path following control of underactuated surface vessels, many of them lack the intuition desired by a control practitioner in terms of tuning controller gains. This issue has motivated the design of the controller presented here. We present a provably stable nonlinear controller for underactuated USVs that provides the intuitive tuning of a PID controller for the yaw angle and a PI controller for the surge velocity. The addition of the integral terms help to add robustness to disturbances and any unmodeled dynamics. As well, we guarantee stability of the closed loop, including boundedness of the unactuated sway mode.

Define the error signals $u_e = u - u_d$, $\psi_e = \psi - \psi_d$, and $r_e = r - r_d$. Then consider the following control law,

$$\begin{aligned}\tau_u = &-K_{Pu}u_e - K_{Iu}\int_{t_0}^{t} u_e(\tau)\,d\tau + m\dot{u}_d + d_{11}u_d \\ &- mr(v + rx_g)\end{aligned} \tag{9}$$

$$\begin{aligned}\tau_r = &-K_{P\psi}\psi_e - K_{I\psi}\int_{t_0}^{t} \psi_e(\tau)\,d\tau - K_{D\psi}r_e \\ &+ \left(I_z - mx_g^2\right)\dot{r}_d + d_{33}r_d - d_{22}vx_g\end{aligned} \tag{10}$$

where K_{Pu}, K_{Iu}, $K_{P\psi}$, $K_{I\psi}$, and $K_{D\psi}$ represent positive control gains that may be tuned by the designer. Application of this control law to the dynamics (3) yields exponential tracking of the desired surge speed and of the desired heading angle. Note that the controller requires the first derivative of desired surge speed as well as the first and second derivatives of desired heading angle. In general, these terms may be generated by passing the reference surge speed and heading angle through suitable low-pass prefilters [4]. When a signal is passed through a low-pass prefilter, the filter states provide a filtered reference signal and its corresponding derivatives. Particularly for the case of desired yaw angle, the prefilter also avoids issues with any discontinuity that may occur in the solution to the closest point on the path to the USV. Passing a potentially discontinuous signal through a low-pass filter will generate a smooth reference signal for tracking. While the effects of saturating actuators are not explicitly considered in the control design, the experimental results confirm the effectiveness of the controller in practice.

This control law consists of proportional and integral terms to stabilize the surge speed, and proportional, integral, and derivative terms to stabilize the heading error. It also contains additional terms to ensure exponential stability of the tracking error dynamics. In this work, a derivative term was not included in the surge speed controller, as in a USV there is already sufficient damping along the surge direction. Stability of the closed loop system with this control law will be shown in the following section.

III. Closed Loop Stability Analysis

The controller presented in this work ensures tracking of surge speed and heading angle in order to accomplish path following. There is no explicit regulation of the position states x and y. As a result, these states are not relevant to the stability analysis. Instead, exponential stability of the tracking error and ultimate boundedness of the sway mode v will be proved. In order to show stability of this system, the following assumption is made.

Assumption 3.1: The reference signals r_d, $\dot{r}_d$, and u_d must be bounded for all time with known bounds.

The following theorems present the main theoretical contribution of this paper, guaranteeing stability of the closed loop system. The first theorem ensures exponential stability of the surge velocity and yaw tracking error dynamics, while the second theorem ensures ultimate boundedness of the sway velocity.

Theorem 3.1: Consider the USV dynamic model (1) and (3) along with control law (9) and (10). The surge speed u and heading ψ will exponentially track the reference surge speed and reference heading if and only if the following conditions are satisfied,

1) $I_z - mx_g^2 > 0$
2) $K_{Iu} > 0$, $K_{Pu} + d_{11} > 0$
3) $K_{P\psi}(d_{33} + K_{D\psi}) - K_{I\psi}(I_z - mx_g^2) > 0$.

Proof: In order to show exponential stability of the surge speed and the heading, additional states for the integrators in the control law must be defined. Define u_{eI} and ψ_{eI} where $\dot{u}_{eI} = u_e$ and $\dot{\psi}_{eI} = \psi_e$. The states under consideration in this analysis are the error dynamics along with the sway velocity state v. Define the state vector under consideration as $x_e = [u_{eI}, u_e, \psi_{eI}, \psi_e, r_e, v]^T$. The error and sway velocity dynamics may then be determined as,

$$\begin{aligned}\dot{u}_{eI} &= u_e \\ \dot{u}_e &= \tfrac{1}{m}\left(\tau_u - d_{11}u\right) + r\left(v + rx_g\right) - \dot{u}_d \\ \dot{\psi}_{eI} &= \psi_e \\ \dot{\psi}_e &= r_e \\ \dot{r}_e &= \frac{(\tau_r - d_{33}r + d_{22}vx_g)}{\left(I_z - mx_g^2\right)} - \dot{r}_d \\ \dot{v} &= -ru - \frac{x_g(m\tau_r - d_{33}mr) + I_z d_{22}v}{m\left(I_z - mx_g^2\right)}.\end{aligned} \tag{11}$$

Applying control law (9) and (10) to the dynamics (11) yields,

$$\dot{x}_e = A_e x_e + g(t, x_e) \tag{12}$$

where A_e is given at the bottom of the following page and $g(t, x_e)$ is defined as,

$$g(t, x_e) = \left[\ 0_{1\times 5}, -r_e u_e - r_e u_d - r_d u_e - r_d u_d - x_g\dot{r}_d\ \right]^T. \tag{13}$$

The term $g(t, x_e)$ is viewed as a nonlinear perturbation term that drives the nominal linear part of system (12). To show exponential stability of the tracking error dynamics,

the matrix A_e must be Hurwitz [11]. Note that this matrix is block diagonal, and as a result the eigenvalues of each of the block sub-matrices may be studied individually to draw conclusions about the whole matrix. From linear systems theory the first block, consisting of the elements in the intersection of the first two rows and columns of A_e, is Hurwitz provided that $(K_{Pu} + d_{11})$, K_{Iu}, and $m > 0$. The physical parameters d_{11} and m will always be greater than zero in practice.

The second block in A_e consists of the intersection of rows 3 to 6 with columns 3 to 6. It is non-trivial to attempt to determine symbolic expressions for the eigenvalues of this sub-matrix. An equivalent but more straightforward approach is to determine the characteristic equation of this sub-matrix and apply the Routh-Hurwitz criteria. Ensuring the characteristic equation is Hurwitz ensures that the sub-matrix is Hurwitz. Applying the Routh-Hurwitz criteria to the characteristic equation of this sub-matrix yields the following conditions,

$$\begin{aligned} I_z - mx_g^2 > 0, \\ K_{P\psi}(d_{33} + K_{D\psi}) - K_{I\psi}(I_z - mx_g^2) > 0. \end{aligned} \tag{14}$$

Choosing the system parameters according to these conditions will ensure that this sub-matrix is Hurwitz. Providing that both blocks are Hurwitz guarantees that A_e is also Hurwitz. Note that the perturbation term does not drive any of the states related to surge speed or heading, and neither are these states affected by the sway velocity v in the closed loop. As a result, the surge speed and yaw error dynamics are globally exponentially stable.

■

The results of this theorem provide intuition in terms of tuning the controller gains. In particular, the presence of integrators in the controller provides some robustness against modeling error and disturbances. However, not all integral gains can be adjusted without regard for system stability. Condition 3) of Theorem 3.1 implies that, while the integral gain on the yaw error may be increased, the derivative gain may also need to be increased in order to ensure that the closed loop system remains stable.

Theorem 3.2: Consider the USV dynamic model (1) and (3) along with control law (9) and (10). If the conditions of Theorem 3.1 are satisfied, the sway velocity v is ultimately bounded.

Proof: To show ultimate boundedness, we use a theorem from Khalil [11, p. 347]. Provided that the conditions of Theorem 3.1 are satisfied, A_e is Hurwitz, and the nominal system is exponentially stable. The following function is a Lyapunov function for the system,

$$V(x_e) = x_e^T P x_e \tag{15}$$

where P is a positive definite matrix satisfying the Lyapunov equation $PA_e + A_e^T P = -Q$, and Q is some positive definite symmetric matrix. Since A_e is Hurwitz, a solution to the Lyapunov equation exists. It can be shown that when the 2-norm is used, the constants from the lemma are given by [11],

$$\begin{aligned} c_1 = \lambda_{\min}(P), \quad c_2 = \lambda_{\max}(P) \\ c_3 = \lambda_{\min}(Q), \quad c_4 = 2\lambda_{\max}(P). \end{aligned} \tag{16}$$

It is also necessary to ensure that the perturbation term $g(t, x_e)$ is bounded with some known upper bound δ. Examining (13), it is clear that each term in the last row is made up either of bounded reference trajectories by Assumption 3.1, exponentially stable error dynamics, or some combination of both. As a result, $g(t, x_e)$ will always be bounded with some upper bound δ. The upper bound will be a function of the initial conditions of the plant, the reference trajectory, and the choice of controller gains. Having established that δ exists, by the lemma, the solution of the perturbed system will be bounded by an exponential until time $t_0 + T$ for some finite T, and bounded by,

$$\|x_e(t)\| \leq b, \ \forall t \geq t_0 + T \tag{17}$$

where,

$$b = \frac{2\lambda_{\max}(P)}{\lambda_{\min}(Q)} \sqrt{\frac{\lambda_{\max}(P)}{\lambda_{\min}(P)}} \frac{\delta}{\theta} \tag{18}$$

for some positive $\theta < 1$. Therefore, ultimate boundedness of the sway velocity v has been established.

■

IV. Simulation Results

The presented path following control algorithm and stability results are now verified through a simulation study. Controller (9) and (10) is applied to USV model (3). The plant parameters are set as $m = 33$ kg, $I_z = 10$ kg m^2, $d_{11} = d_{22} = d_{33} = 5$ N s/m, and $x_g = 0.1$ m. The controller gains are set as $K_{Pu} = 5$, $K_{Iu} = 0.5$, $K_{P\psi} = 5$, $K_{I\psi} = 0.1$, $K_{D\psi} = 1$. These choices of gains satisfy the conditions of Theorem 3.1. The path for the USV to follow is defined as a clockwise circle centred at the origin with a radius of 4 m. The desired surge velocity of the boat is set initially as 0.1 m/s, and then increased to 0.2 m/s 100

$$A_e = \begin{bmatrix} 0 & 1 & 0 & 0 & 0 & 0 \\ -\frac{K_{Iu}}{m} & -\frac{(K_{Pu}+d_{11})}{m} & 0 & 0 & 0 & 0 \\ 0 & 0 & 0 & 1 & 0 & 0 \\ 0 & 0 & 0 & 0 & 1 & 0 \\ 0 & 0 & -\frac{K_{I\psi}}{I_z - mx_g^2} & -\frac{K_{P\psi}}{I_z - mx_g^2} & -\frac{(K_{D\psi}+d_{33})}{I_z - mx_g^2} & 0 \\ 0 & 0 & \frac{x_g K_{I\psi}}{I_z - mx_g^2} & \frac{x_g K_{P\psi}}{I_z - mx_g^2} & \frac{x_g (K_{D\psi}+d_{33})}{I_z - mx_g^2} & -\frac{d_{22}}{m} \end{bmatrix}$$

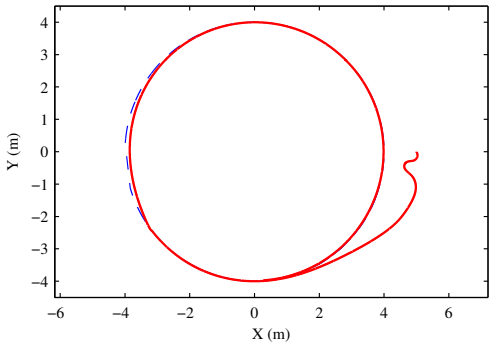

Fig. 1. Desired path (dashed) and trajectory of USV (solid) converging to and driving along desired path.

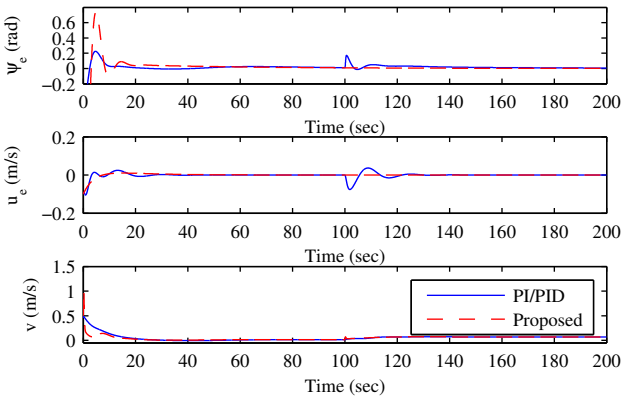

Fig. 2. Yaw tracking error ψ_e, surge velocity tracking error u_e, and sway velocity v. Dashed lines show results from controller presented here, while solid lines show results from a PI controller for surge velocity and a PID controller for yaw.

seconds into the simulation. The initial state of the USV was set to $\eta = [5, 0, -2.8274]^T$ and $\nu = [-0.1, 0.5, 0]^T$, with linear units of m and m/s and angular units of rad and rad/s. The dynamics in the simulation are numerically integrated using a first order Runge-Kutta solver with a sample period of $T_s = 0.01$ seconds.

Fig. 1 shows the desired circular path and the trajectory taken by the USV to get onto the path and drive around it. At roughly (-3.2 m, -2.4 m) on the path, the step change in velocity occurs. In order to ensure accurate path following, the value of the "carrot point" is adjusted here. Since it takes some time for the actual surge velocity to reach the new value of 0.2 m/s, the boat deviates slightly from the path for a short period of time. Examining Fig. 2, the states stabilized by the controller can be seen and are represented by the dashed lines. As explained by the theory, the yaw tracking error and the surge velocity tracking error are exponentially stable. It is as a result of this that the USV is able to reach the path and drive on it. As well, the unactuated sway velocity is seen in this plot to be bounded. The solid lines represent a simulation where the nonlinear terms in the controller are not included. This simplified controller is a PI loop around surge velocity and a PID loop around yaw. It is clear that the nonlinear controller presented here outperforms the simpler

Fig. 3. The Clearpath Kingfisher M100 USV used in this work.

approach. When the step change in desired velocity occurs, the controller presented here is able to track it exactly, while the simpler controller lacking the nonlinear terms experiences a transient in the surge velocity tracking error that lasts roughly 20 seconds. With higher gains for the simpler controller, the magnitude of the transient could be reduced, but not completely eliminated. While difficult to see in this plot, the yaw tracking error experiences a transient at the same point in time for the case of the simpler controller, but the nonlinear controller does not.

V. Experimental Results

The control law presented in this work is implemented on a Clearpath Robotics Kingfisher M100 platform, shown in Fig. 3. The Kingfisher is a small (33 kg) USV propelled by two electric trolling motors mounted in pods on either side of the craft, and set up in a differential drive configuration. It is equipped with a GPS receiver for global position measurements and a digital compass unit to provide heading measurements. The position measurements are sampled at 10 Hz, while the orientation is measured at a rate of 20 Hz.

Since the control algorithm presented requires knowledge of the local velocity states, an extended Kalman filter (EKF) is used, based on the dynamics (1) and (3) and driven by the global position and orientation measurements. The EKF, as well as the controller dynamics, are run at 100 Hz.

A system identification was performed for this USV using measurements collected through several trajectories remotely commanded by an operator through radio-control. The identified parameters are then used in the control law to compensate for the plant nonlinearities. Consequently, the proposed controller is critically dependent on the accuracy of these plant parameters. The low quality of the onboard measurements leads to a significant amount of modeling error. Additionally, the dynamic model does not capture all of the nonlinear hydrodynamic effects caused by different boat speeds, such as wake effects or hull planing. However, these errors should be attenuated by the residual PI and PID controllers on the surge speed and yaw angle, respectively.

The implementation was tested on a small lake where the USV was commanded to drive a sinusoidal path with an amplitude of 12 m and a period of 40 m. The desired surge speed was set to 0.4 m/s. The resulting path traversed for this trial is shown in Fig. 4.

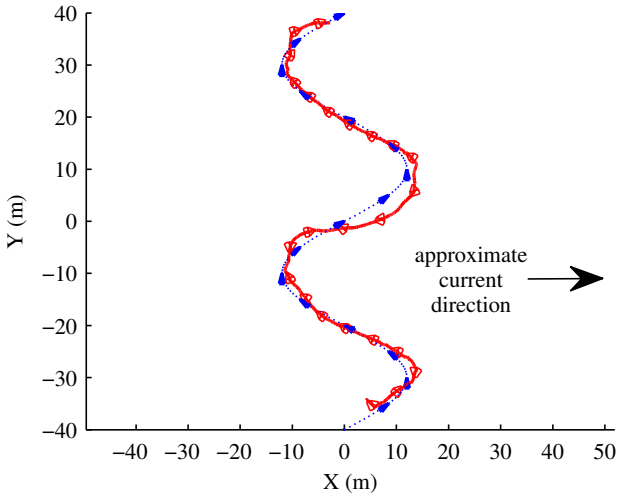

Fig. 4. Desired path (dotted) and trajectory of USV (solid) along commanded sinusoidal path measured in experiment using proposed controller.

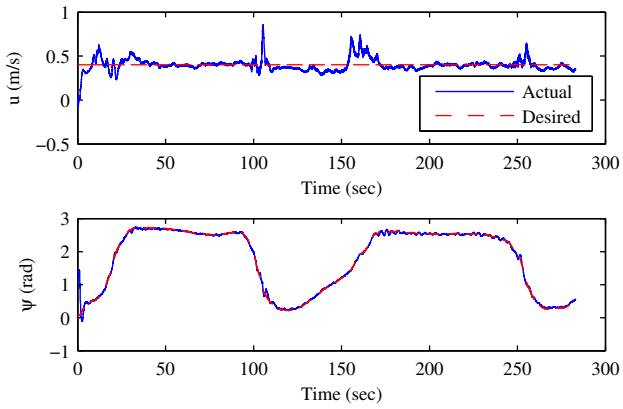

Fig. 5. Actual (solid) and desired (dashed) values for USV surge speed (top) and yaw angle (bottom) in experiment run using proposed controller.

A particularly large current disturbance can be observed through the second counter-clockwise turn. In this case, the current disturbance velocity is large with respect to the desired surge speed of the vessel. However, the USV does recover the path-following on the straight portion. The resulting errors on surge speed and yaw angle are shown in Fig. 5.

The slow reconvergence to the path is partially affected by the choice of $\Delta\theta$. A smaller value would allow for faster convergence, but would amplify errors on the EKF position and orientation estimates, while a large value smooths out the noise, but causes slower convergence to the path, particularly in regions of high curvature.

VI. Conclusion

This work has presented a new path following control algorithm for unmanned surface vessels. The algorithm has the dual benefits of being provably stable and intuitive to tune. A stability analysis was performed showing that exponential convergence of the surge velocity and the vehicle heading to desired values can be guaranteed, while ultimate boundedness of the unactuated sway velocity has been proved. In order to accomplish path following, a desired heading is generated by determining the closest point on the desired path to the vehicle, and computing the heading angle between the vehicle and a point some distance ahead of the closest point.

The controller contains PID terms for the heading, and PI terms for the surge speed. These terms allow intuitive tuning of the controller in practice – something that is of great benefit to control practitioners, and in addition the integral terms provide some level of robustness to disturbances and unmodeled dynamics. Simulation results were presented, confirming the theoretical results in the ideal case. Finally, the controller was implemented on the Clearpath Robotics Kingfisher M100 and verified experimentally outdoors using GPS and compass measurements. The experimental results have shown the feasibility of the approach in practice, where modeling error, sensor noise, and external disturbances are factors.

Future work in this area will focus on several topics, including the estimation and rejection of current disturbances, development of a unified control strategy that accomplishes both path following and station keeping, as well addition of a vision sensor to improve the quality of the measurements when operating outdoors. Additionally, approaches to determine the "carrot point" based on the desired surge speed and path shape will be examined.

References

[1] P. Krishnamurthy, F. Khorrami, and S. Fujikawa, "A modeling framework for six degree-of-freedom control of unmanned sea surface vehicles," in *44th IEEE Conference on Decision and Control, and the European Control Conference 2005*. Seville, Spain, Dec. 2005, pp. 2676–2681.

[2] J. Ghommam, F. Mnif, and N. Derbel, "Global stabilisation and tracking control of underactuated surface vessels," *Control Theory & Applications, IET*, vol. 4, no. 1, pp. 71–88, 2010.

[3] T. Fossen, S. Sagatun, and A. Sørensen, "Identification of dynamically positioned ships," *Control Engineering Practice*, vol. 4, no. 3, pp. 369–376, 1996.

[4] T. Fossen, M. Breivik, and R. Skjetne, "Line-of-sight path following of underactuated marine craft," in *Proceedings 2003 IFAC Conference on Maneuvering and Control of Marine Craft*, 2003.

[5] M. Bibuli, G. Bruzzone, M. Caccia, G. Indiveri, and A. Zizzari, "Line following guidance control: Application to the charlie unmanned surface vehicle," in *Intelligent Robots and Systems, 2008. IROS 2008. IEEE/RSJ International Conference on*. IEEE, 2008, pp. 3641–3646.

[6] M. Bibuli, G. Bruzzone, M. Caccia, and L. Lapierre, "Path-following algorithms and experiments for an unmanned surface vehicle," *Journal of Field Robotics*, vol. 26, no. 8, pp. 669–688, 2009.

[7] M. Caccia, M. Bibuli, R. Bono, and G. Bruzzone, "Basic navigation, guidance and control of an unmanned surface vehicle," *Autonomous Robots*, vol. 25, no. 4, pp. 349–365, 2008.

[8] R. Skjetne, Ø. Smogeli, and T. Fossen, "A nonlinear ship manoeuvering model: Identification and adaptive control with experiments for a model ship," *Modeling, Identification and control*, vol. 25, no. 1, pp. 3–27, 2004.

[9] M. Breivik and T. Fossen, "Path following for marine surface vessels," in *OCEANS'04. MTTS/IEEE TECHNO-OCEAN'04*, vol. 4. IEEE, 2004, pp. 2282–2289.

[10] M. Breivik, "Nonlinear maneuvering control of underactuated ships," *Master's thesis, NTNU, Trondheim, Norway*, 2003.

[11] H. K. Khalil, *Nonlinear Systems*, 3rd ed. New Jersey: Prentice Hall Inc., 2002.